Quantitative and Topographical Analysis of the Losses of Cone Photoreceptors and Retinal Ganglion Cells Under Taurine Depletion

Wahiba Hadj-Saïd,[1–3] Nicolas Froger,[1–3] Ivana Ivkovic,[1–3] Manuel Jiménez-López,[4] Élisabeth Dubus,[1–3] Julie Dégardin-Chicaud,[1–3] Manuel Simonutti,[1–3] César Quénol,[1–3] Nathalie Neveux,[5,6] María Paz Villegas-Pérez,[4] Marta Agudo-Barriuso,[4] Manuel Vidal-Sanz,[4] Jose-Alain Sahel,[1–3,7–9] Serge Picaud,[1–3] and Diego García-Ayuso[4]

[1]INSERM U968, Institut de la Vision, Paris, France
[2]Sorbonne Universités, UPMC Univ Paris 06, UMR_S968, Institut de la Vision, Paris, France
[3]CNRS UMR7210, Institut de la Vision, Paris, France
[4]Departamento de Oftalmología, Facultad de Medicina, Universidad de Murcia, Murcia, Spain and Instituto Murciano de Investigación Biosanitaria- Hospital Virgen de la Arrixaca (IMIB-Arrixaca)
[5]Service de Biochimie, Groupe Hospitalier Cochin – Hôtel-Dieu, Assistance Publique – Hôpitaux de Paris, Paris, France
[6]Laboratoire de Nutrition, EA 4466, Université Paris Descartes, Faculté de Pharmacie, Paris, France
[7]CHNO des Quinze-Vingts, Paris, France
[8]Academie des Sciences, Paris, France
[9]Fondation Ophtalmologique Adolphe de Rothschild, Paris, France

Correspondence: Serge Picaud, UPMC Univ Paris 06, Institut de la Vision, UMR_S 968, F-75012, Paris, France; serge.picaud@inserm.fr.
Diego García-Ayuso, Laboratorio de Oftalmología Experimental, Instituto Murciano de Investigación Biosanitaria-Virgen de la Arrixaca, Edificio LAIB Planta 5a, Carretera Buenavista s/n, 30120 El Palmar, Murcia, Spain; diegogarcia@um.es.

Submitted: March 10, 2016
Accepted: July 29, 2016

Citation: Hadj-Saïd W, Froger N, Ivkovic I, et al. Quantitative and topographical analysis of the losses of cone photoreceptors and retinal ganglion cells under taurine depletion. *Invest Ophthalmol Vis Sci*. 2016;57:4692–4703. DOI:10.1167/iovs.16-19535

Purpose. Taurine depletion is known to induce photoreceptor degeneration and was recently found to also trigger retinal ganglion cell (RGC) loss similar to the retinal toxicity of vigabatrin. Our objective was to study the topographical loss of RGCs and cone photoreceptors, with a distinction between the two cone types (S- and L- cones) in an animal model of induced taurine depletion.

Methods. We used the taurine transporter (Tau-T) inhibitor, guanidoethane sulfonate (GES), to induce taurine depletion at a concentration of 1% in the drinking water. Spectral-domain optical coherence tomography (SD-OCT) and electroretinograms (ERG) were performed on animals after 2 months of GES treatment administered through the drinking water. Retinas were dissected as wholemounts and immunodetection of Brn3a (RGC), S-opsin (S-cones), and L-opsin (L-cones) was performed. The number of Brn3a$^+$ RGCs, and L- and S-opsin$^+$ cones was automatically quantified and their retinal distribution studied using isodensity maps.

Results. The treatment resulted in a significant reduction in plasma taurine levels and a profound dysfunction of visual performance as shown by ERG recordings. Optical coherence tomography analysis revealed that the retina was thinner in the taurine-depleted group. S-opsin$^+$cones were more affected (36%) than L-opsin$^+$cones (27%) with greater cone cell loss in the dorsal area whereas RGC loss (12%) was uniformly distributed.

Conclusions. This study confirms that taurine depletion causes RGC and cone loss. Electroretinograms results show that taurine depletion induces retinal dysfunction in photoreceptors and in the inner retina. It establishes a gradient of cell loss depending on the cell type from S-opsin$^+$cones, L-opsin$^+$cones, to RGCs. The greater cell loss in the dorsal retina and of the S-cone population may underline different cellular mechanisms of cellular degeneration and suggests that S-cones may be more sensitive to light-induced retinal toxicity enhanced by the taurine depletion.

Keywords: taurine, photoreceptor, retinal ganglion cell, retinal degeneration, light, albino

Nutritional depletion of taurine causes the degeneration of photoreceptors in cats.[1] Various studies have investigated the role of taurine in retinal diseases affecting photoreceptors, such as retinitis pigmentosa (see below). It was shown that taurine supplementation added to diltiazem and vitamin E improves photoreceptor survival in this disease.[2] However, no study has demonstrated taurine deficiency in this hereditary disease.[3–5] Taurine is present at high levels in tissues such as eyes and muscles and taurine uptake can vary greatly according to diet.[6] Its importance for the human retina was demonstrated by the observation of a functional deficit in patients receiving parenteral nutrition lacking taurine.[7,8] We recently discovered that patients treated with vigabatrin for infantile spasms show a decrease of their plasma taurine concentration.[9] This may explain the visual constriction observed in vigabatrin-treated patients.[10] The toxicity of the molecule was attributed, not only

to photoreceptor loss, but also to a primary lesion at the site of retinal ganglion cells (RGC) leading to the loss of optic fibers.[11–14]

Following the initial discovery in cats,[1] a taurine-free diet was also found to generate photoreceptor lesions in baby monkeys.[15] Pharmacological treatment was required to produce taurine depletion in rodents and induce photoreceptor degeneration.[16] The genetic invalidation of the taurine transporter (Tau-T) in knock-out mice also resulted in substantial photoreceptor degeneration.[17] We have observed cone loss prior to rod alterations in animal studies to examine the retinal toxicity of the antiepileptic drug vigabatrin.[9] Clinical reports of a primary lesion site in RGCs led us to examine the fate of these cells in vigabatrin-treated rats. We found that RGCs degenerate in vigabatrin-treated rats and that taurine supplementation prevents this RGC loss.[18] The parallel degeneration of cone photoreceptors and RGCs was also observed under taurine depletion generated in mice fed with guanidoethane sulfonate (GES), a taurine transporter blocker.[19] The direct effect of taurine on RGCs was then demonstrated using pure RGC cultures and different models of RGC degeneration.[6] Taurine depletion acts synergistically with light to trigger the photoreceptor lesion[9,20–22] and photoreceptor loss appears to be more severe in the dorsal area, as it does for light damage.[23–25] However, these studies did not include RGC counts and the conclusions were drawn from data based on retinal sections alone. This study[19] considered the whole cone cell populations irrespectively of the S- or L-opsin specificity and the asymmetric dorsoventral distributions of these cone subtypes. In the present study, we have examined the distribution of cell loss for S- and L-cones and RGCs under taurine deficiency induced by the administration of GES through the drinking water.

Methods

Animals and Treatment

Two-month-old male BALB/cJRj mice (Janvier, Saint Isle, France) were divided into a control group of mice drinking GES-free water (Control group) and a group of mice treated with GES (Toronto research chemical Inc., North York, ON, Canada) through the drinking water at a concentration of 1% for 2 months (GES-treated group).[19] Both groups of mice were provided with laboratory chow and tap water ad libitum. Animals were maintained on a 12 hour light/12 hour dark (LD) cycle under standard lighting conditions (85 lux) below the lamps in the center of the room and 5 lux in the individual cages. All experiments were carried out in accordance with the European Community Council Directives (86/609/EEC) and with the ARVO statement for the Use of Animals in Ophthalmic and Visual Research.

SD-OCT Imaging

Spectral-domain optical coherence tomography (SD-OCT) was performed on both eyes and averaged from each animal after 2 months of GES treatment. The pupils were dilated with Tropicamide (Mydriaticum, Théa, France) and phenylephrine (Néosynephrine, Europhta, France). The animals were anesthetized by inhalation of Isoflurane (Axience, Paris, France) and placed in front of the SD-OCT imaging device (Bioptgen 840 nm HHP; Bioptgen, Durham, NC, USA). The eyes were kept moist with 9% NaCl during the whole procedure. Image acquisitions were performed using the following parameters: rectangular scan/1000 A-scan per B-scan/100B-scan 1 frame or 4B-scans 16 frames. The acquired images were saved as .AVI files and processed using Fiji software (in the public domain, at http://fiji.sc/Fiji). The thickness of retinal layers was manually measured on maximum projection images in an axis perpendicular to the individual layers and 500 μm from the center of the optic nerve.[26]

Electroretinograms

Electroretinograms (ERG) were performed on all mice from the two experimental groups (Control and GES-treated). After overnight dark adaptation, the mice were anesthetized with ketamine (100 mg/kg; Virbac, Carros, France) and Xylazine (10 mg/kg; Axience, Pantin, France). Eye drops were used to dilate the pupils (0.5% tropicamide) and anesthetize the cornea (0.4% oxybuprocaine chlorhydrate). The body temperature was maintained at 37°C using a heating pad. The upper and lower lids were retracted to keep the eyes open and bulging. Custom-made gold contact lens electrodes were placed on the corneal surface to record the ERG (Espion; Diagnosys LLC, Littleton, MA, USA). Needle electrodes placed subcutaneously in cheeks served as reference and a needle electrode placed in the back served as ground. Recordings were made from both eyes, simultaneously, and measures were averaged for each animal. The light stimulus was provided by a Ganzfeld stimulator (Espion, Diagnosys LLC, Littleton, MA, USA). The responses were amplified and filtered (1-Hz low and 300-Hz high cut off filters) with a 1-channel DC-/AC-amplifier.

Two levels of stimulus intensity of 3 and 10 cd.s.m^2 were used for the dark-adapted ERG recorded. Each scotopic ERG response represents the average of five responses from a set of five stimulation flashes. To isolate cone responses, a 5-minute light adaptation at 20 cd.m^2 was used to saturate rod photoreceptors. A stimulus intensity of 10 cd.s.m^2 was used for the light-adapted (photopic) ERGs. Flicker light stimulation was performed at 10 Hz and the responses were averaged over a 40-second stimulation period. Each scotopic, photopic, and flicker response represents the average of 10 measures. The major components of the ERG were measured conventionally.[27] All comparisons were performed at an intensity of 10 cd.s.m-^{2} (scotopic and photopic responses).

Blood and Tissue Samples

Animals were anaesthetized with ketamine (100 mg/kg; Virbac) and Xylazine (10 mg/kg; Axience). Blood samples were collected in hemolysis tubes containing heparin (14 IU/ml). After centrifugation, plasma was removed and frozen at −20°C until used for amino acid analysis.

The animal was transcardially perfused with 4% paraformaldehyde (PFA) in PBS (0.01 M, pH 7.4) after a saline rinse. Just after deep anesthesia, a suture was placed on the dorsal pole of each eye. Retinas were dissected as wholemounts by making four radial cuts (the deepest one in the dorsal pole), post fixed for an additional hour in 4% PFA and kept in PBS until further processing. For cross-sectional analysis, eyes were enucleated, then the cornea, iris, and lens were removed and eyecups were cryoprotected following previously described methods.[19]

Plasma Taurine Level

Samples were deproteinized with a 30% (wt/vol) sulfosalicylic acid solution and the supernatants stored at −80°C until analysis. Amino acids were measured by ion exchange chromatography with ninhydrin detection after dilution of the samples with a lithium citrate buffer containing D-glucosaminic acid and amino-ethylcysteine as internal standards using an amino acid analyzer (AminoTac, JLC-500/V; Jeol, Tokyo, Japan).[28] The results of our participation in the

Table. Antibodies Used

Primary Antibodies	Secondary Antibodies (1/500; Molecular Probes, Invitrogen, Carlsbad, CA, USA)
• S-opsin: goat anti-OPN1SW, 1:1,000 (ref: sc-14365; Santa Cruz, CA, USA). • L-opsin: rabbit anti-opsin antibody, red/green, 1:500 (ref: AB5405; Merck Millipore, Darmstadt, Germany). • Brn3a: mouse anti-Brn3a, 1:100 (ref: MAB1585; Chemicon, Temecula, CA, USA). • Rabbit anti-cone-arrestine, 1:20000 (ref: AB15282; Chemicon).	• donkey anti-goat Alexa Fluor 488. • donkey anti-rabbit Alexa Fluor 594. • donkey anti-mouse Alexa Fluor 594. • donkey anti-rabbit Alexa Fluor 488.

European Quality Control Scheme (ERNDIM, Maastricht, the Netherlands) indicate the accuracy of our amino acid determinations.

Immunohistochemistry

After permeabilization and saturation, retinal wholemounts and cross-sections were incubated first with primary antibodies overnight and then with secondary antibodies for 1 hour. After washing, retinas were flat-mounted on slides. The left eye from each animal was used to study the RGC population, and the right eye was used to study cone population. For retinal cross-sections, cell nuclei were revealed incubating them with 4′,6-diamidino-2-phenylindole (10 μg/mL; DAPI, Sigma-Aldrich, St. Louis, MO, USA). Inner/outer segments of cone photoreceptors were stained with a peanut agglutinin lectin conjugated to Alexa Fluor 594 (PNA, 1:40; Molecular Probes, Invitrogen, Carlsbad, CA, USA) overnight at 4°C. Sections were then rinsed and mounted with Permafluor reagent (Microm, Francheville, France). The antibodies are described in the Table.

Image Acquisition

Each retinal wholemount was acquired using an Inverted Microscope, (Nikon Eclipse Ti; Nikon, Tokyo, Japan) controlled by Metamorph software (Molecular Devices, Sunnyvale, CA, USA) in multiple frames. Individual frames were tiled to reconstruct the wholemounts using Metamorph software.

Retinal cross-sections were acquired using an Olympus FLUOVIEW FV1000 confocal laser scanning microscope (Olympus, Tokyo, Japan).

Automatic Quantification of the Total Population of Brn3a-Positive RGCs in Wholemounted Retinas

The individual fluorescent images taken from each retinal wholemount were processed with a specific adaptation of the previously published cell-counting routine[29] to automatically quantify Brn3a$^+$ RGCs in naïve and injured retinas. Briefly, we used the IPP macro language to apply a sequence of filters and transformations to each image to clarify cell limits and separate individual cells for automatic cell counting.

This new adaptation of the Brn3a automatic counting method was validated by having three different experienced investigators manually count, in a masked fashion, a total of 16,719 Brn3a$^+$ RGCs present in 10 frames, representing different RGC density regions, which were randomly selected from nine wholemounted naïve and experimental retinas. These results were plotted against the counts obtained automatically (15,922 cells). There was a strong correlation between both methods (Pearson correlation test, r^2=0.965) thus validating the automatic quantification of Brn3a$^+$ RGCs.

Automatic Quantification of the Total Population of S-opsin$^+$ and L-opsin$^+$cones in Wholemounted Retinas

Automated counting routines were adapted in a single counting routine to quantify the S-opsin$^+$ and L-opsin$^+$ cones. This routine quantified positive cell segments present in the retina. This routine has been previously described in detail.[30]

The adaptation of the counting method was validated by having three different experienced investigators manually count, in a masked fashion, a total of 42,710 segments present in 20 frames, representing different cone density regions, which were randomly selected from eight wholemounted naïve and experimental retinas. These results were plotted against the counts obtained automatically (43,156 cells). There was a strong correlation between both methods (Pearson correlation test, $r^2 = 0.915$) thus validating the automatic quantification of cone segments.

Isodensity Maps

The detailed spatial distribution of Brn3a$^+$ RGCs and S- and L-cones over the entire retina was obtained through quadrant analysis, and demonstrated using isodensity maps constructed as previously described.[30,31] The only difference was that each frame was divided into 16 areas of interest instead of 36; the studied quadrants had an area of 0.03 mm^2.

Statistical Analysis

All data are expressed as the mean ± SEM. Statistical analysis was performed using Sigma Stat 3.1 for Windows (Sigma Stat for Windows TM version 3.11; Systat Software, Inc., Richmond, CA, USA) or GraphPad Prism (GraphPad Prism Software, Inc. San Diego, CA, USA). For retinal populations, the ANOVA test followed by Tukey's post hoc test was used when comparing more than two groups, and the Mann-Whitney *U* or *t*-test were used when comparing only two groups. For plasma, OCT, and ERG, statistical comparisons were performed using either the unpaired Student's *t*-test or nonparametric Mann-Whitney *U* test. Differences were considered to be significant when *P* less than 0.05.

Results

Taurine Plasma Levels

Guanidoethane sulfonate is a known blocker of the Tau-T. We measured taurine levels in the plasma collected when the animals were killed to verify the efficacy of GES administration. In GES-treated mice, the plasma taurine levels were significantly lower relative to those in untreated control animals ($P <$ 0.0001; Fig. 1). This result confirms the efficacy of the GES treatment on taurine distribution.

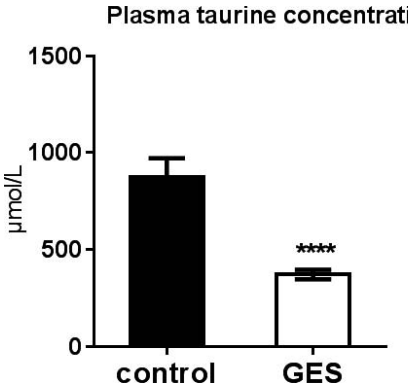

FIGURE 1. Plasma taurine concentration. Plasma taurine concentration after 2 months of treatment with GES, administrated in the drinking water (*white bar*; $n = 16$), relative to control mice drinking GES-free water (*black bar*; $n = 15$).

Retinal Function

Retinal cell function was investigated in GES-treated animals by ERG recordings. Under scotopic conditions (flashes of 10 cd.s/m^2), the ERG a-wave signal provides an in vivo measure of the dynamic response from rod photoreceptors whereas the ERG b-wave-signal provides information about activity in the inner retina. After 2 months of GES treatment; the a-wave amplitude was reduced by 23% indicating moderate dysfunction of rod photoreceptors (GES-treated group: 114.1 ± 8.5 µV, $n = 12$; control group: 149.6 ± 12.9 µV, $n = 10$, $P = 0.0169$; Fig. 2A). The amplitudes of the ERG b-wave were reduced by 60% in the GES-treated group (GES group: 123.4 ± 67.7 µV, $n = 12$; control group: 312.5 ± 80.9 µV, $n = 11$, $P < 0.0001$; Fig. 2B), suggesting a stronger effect of the treatment on the inner retina. Photopic ERG recordings were also performed to assess the function of the cone pathway. Light flashes (10 cd.s/m^2) were applied on a background light used to saturate rod photoreceptors. In GES-treated animals, amplitudes of the photopic ERG were significantly decreased by 53% when compared with nontreated, control mice (GES group: 20 ± 3.9 µV, $n = 12$; control group: 42.6 ± 4.7 µV, $n = 10$, $P = 0.0026$; Fig. 2C). We measured responses to flickering light, which cannot be followed by rod photoreceptors, to further confirm this dysfunction in the cone pathways in the GES-treated animals. A significant decrease (47%) in the amplitudes of the 10-Hz flicker response was observed in GES-treated mice relative to nontreated, control mice (GES group: 9.3 ± 1.1 µV, $n = 12$; control group: 17.8 ± 2.1 µV, $n = 10$, $P < 0.0012$; Fig. 2D). These results confirm that administration of GES in the drinking water, and consequent taurine depletion, induce retinal dysfunction and may lead to functional changes of the inner retina.

In Vivo Retinal Thickness

We examined the retina of living animals with an SD-OCT to see if the functional deficit was associated with changes

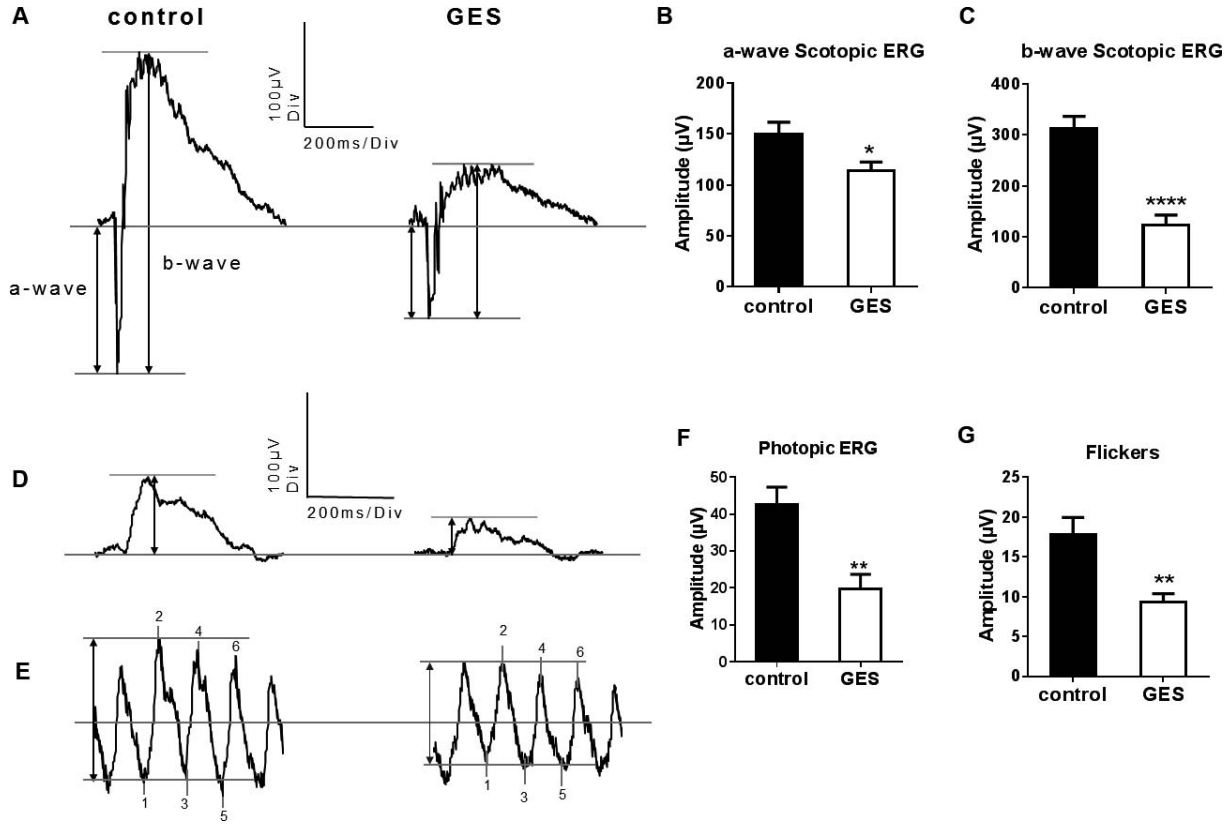

FIGURE 2. Taurine depletion induced functional deficit in the retina. (**A**) Scotopic ERG recordings showing a decreased amplitude in a GES-treated mouse compared with a control mouse. (**B**, **C**) Quantifications of scotopic a-wave (**B**) and b-wave amplitudes (**C**) showing significant decreases in GES treated mice. (**D**) Photopic ERG recordings showing a decreased ERG response in a GES-treated mouse compared with a control mouse. (**F**) Quantification of photopic ERG amplitudes showing a significant decrease in GES treated mice. (**E**) Flickers ERG recordings showing a decreased ERG response in a GES-treated mouse compared with a control mouse. (**G**) Quantification of flicker response amplitudes showing a significant decrease in the GES-treated mice. These functional results suggest that cone population is affected. (****$P < 0.0001$; **$P < 0.002$; *$P < 0.05$, nonparametric Mann-Whitney *U* test).

Investigative Ophthalmology & Visual Science

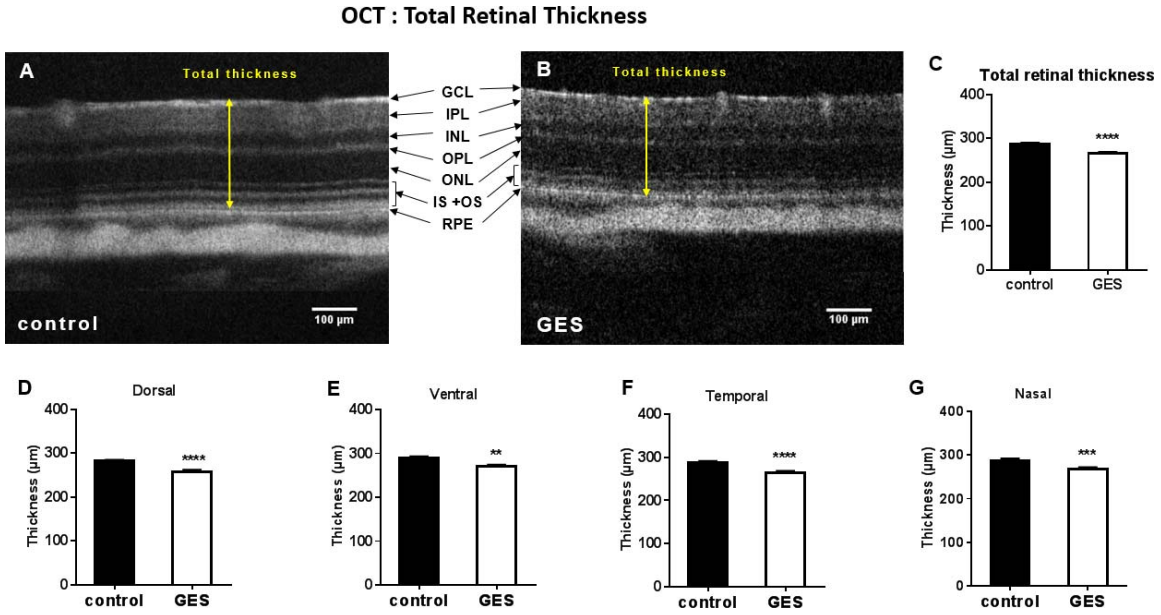

FIGURE 3. Retinal thickness studied by OCT. Representative images from the in vivo OCT scan of a control (**A**) and GES-treated retina (**B**). Histograms showing the total retinal thickness in the whole retina (**C**) and in the dorsal (**D**), ventral (**E**), nasal (**F**), and temporal (**G**) quadrants of the retina in control and GES-treated mice. (****$P < 0.0001$; ***$P < 0.001$; **$P < 0.002$, nonparametric Mann-Whitney U test; $n = 10$–12).

detectable in vivo. After 2 months of GES treatment, the retina was significantly thinner relative to the retinal thickness in nontreated, control mice (GES group: 265.6 ± 2.8 nm, $n = 12$; control group: 287.1 ± 2.6 nm, $n = 10$, $P < 0.0001$; Fig. 3). The measurement was reiterated in each quadrant to see whether the retinal thinning preferentially affected a specific quadrant or the whole retina. We observed the decrease in thickness in all quadrants indicating a homogeneous change throughout the retina. The reduction of the RNFL thickness was also analyzed with SD-OCT, but we found no significant differences (data not shown).

Total Population and Spatial Distribution of Cones

Our previous study had reported a loss of cone photoreceptors on retinal sections.[19] This cell count did not provide an overview of the cellular loss or specify if one population of cones was more affected than the other. We thus immunolabelled the retina for the S-opsin$^+$ and L-opsin$^+$ cones to quantify the numbers of both populations in GES-treated and nontreated, control animals. This allowed us to build isodensity maps of both cone populations (please see references above) in which densities are translated into colors using a scale that goes from purple (0 cones/mm^2) to red (the maximum), according to the population studied. Automatic quantification of the total population of L-opsin$^+$ and S-opsin$^+$ cones revealed that, in the BALB/c strain, the number of cones expressing S-opsin is higher than those expressing L-opsin in nontreated mice (Figs. 4A–C, 4E, 5A–C, 5E). The topography of S-cones in the nontreated, control animals showed a higher density in the ventronasal region of the retina, which gradually decreases along a gradient toward the dorsotemporal region of the retina (Fig. 4C). The higher number of S-opsin$^+$cones and their topography are in accordance with previous studies performed in other strains of albino mice (Figs. 4A–C, 4E, 5A–C, 5E).[30,32]

Isodensity maps for GES-treated animals showed a decrease in warm colors throughout the retina relative to untreated animals, but mainly in the dorsotemporal region of the retina (Fig. 4D). This suggests that the decrease of S-opsin$^+$ cones is higher in the dorsal retina in the taurine depleted animals. We quantified the loss of S-opsin$^+$ cones over the entire retina, showing a 36% decrease for the GES-treated animals relative to control mice (Control: 119,182 ± 13,392 S-opsin$^+$ cones [$n = 11$]; GES-treated 75,690 ± 11,086 S-opsin$^+$ cones [$n = 11$]). This difference was statistically significant ($P < 0.05$).

The topography of L-opsin$^+$cones showed a higher density around the optic nerve that decreased gradually from the center to the periphery with a slightly greater density in the dorsal retina. This distribution is similar to that observed in previous studies in naïve animals from albino strains (Figs. 5A–C).[30] We observed a greater decrease in warm colors in the dorsal region of the retina in the GES-treated animals (Fig. 5D) suggesting that the decrease of L-opsin$^+$ cones is higher in this region of the retina in the taurine-depleted animals. We quantified the loss of L-opsin$^+$ cones over the entire retina of the GES-treated animals, showing a significant difference of 27% relative to the control animals (Control: 101,140 ± 12,790 L-opsin$^+$ cones [$n = 11$]; GES: 73,417 ± 17,008 L-opsin$^+$ cones [$n = 11$]). These results suggest that S-opsin$^+$ cones appear to be more sensitive to taurine deprivation than L-opsin$^+$ cones even if both populations are affected.

Cone Morphologic Changes

To study further the dysfunction of cone photoreceptors, we performed immunolabeling on retinal cross-sections against another protein involved in cone light response, the cone arrestine. Figure 6 illustrates the change in cone arrestine distribution in the retina of GES-treated animals. First, the number of cone photoreceptors appeared reduced in the GES-treated animals compared with control (Figs. 6A, 6B) as demonstrated above with the cell counting. More importantly, the immunostaining of cone outer segments was less regular and straight than in control animals and the staining of cone synaptic terminals became shrunk and irregular (Figs. 6A, 6B). By contrast, the PNA staining of the cone outer segment extracellular matrix seemed morphologically unchanged although reduced in number (Fig. 6C, 6D). On these retinal sections, the retinal thickness was not greatly modified as

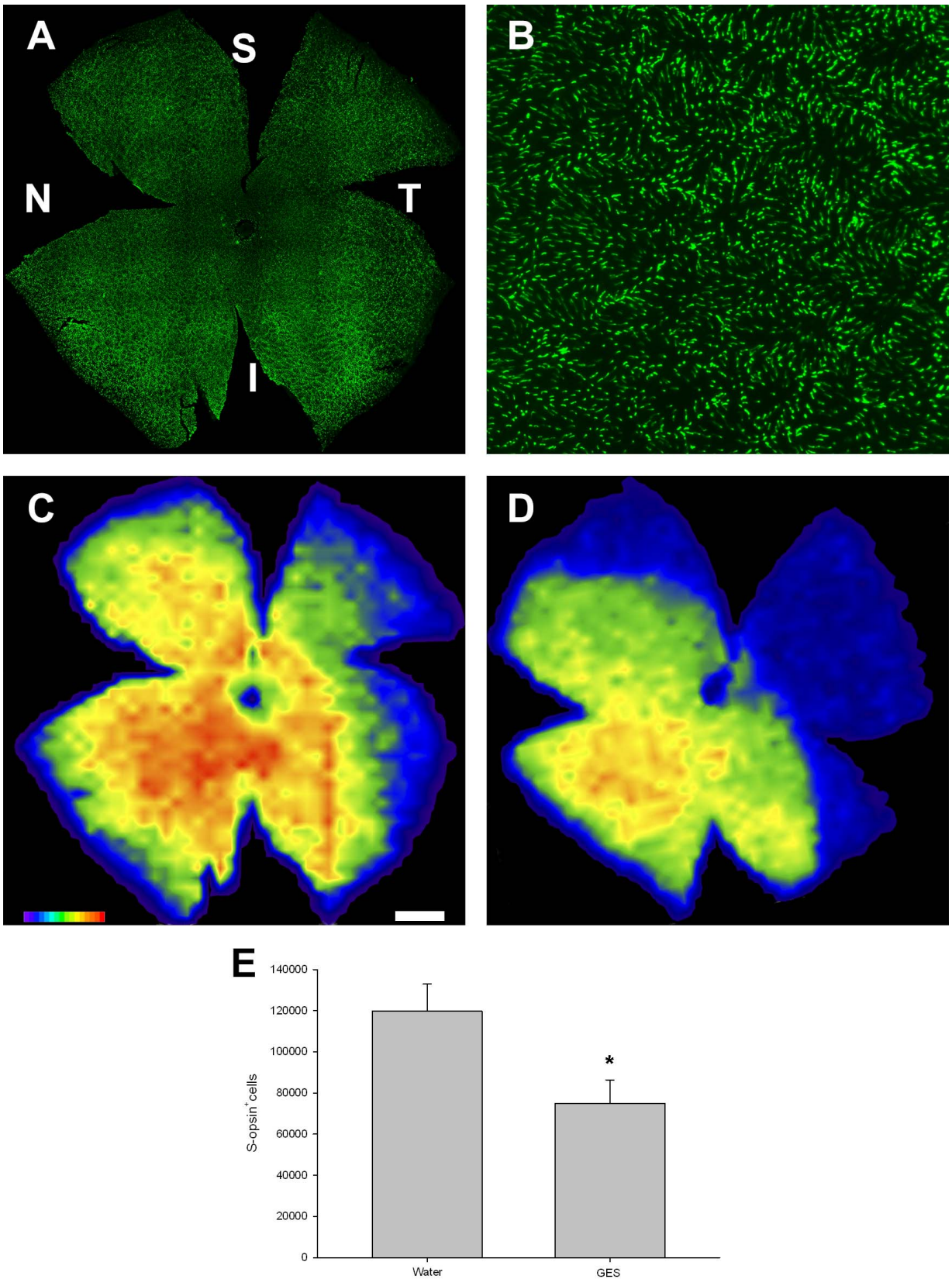

FIGURE 4. Loss of S-opsin$^+$cones in taurine-depleted mice. (**A**) Representative retina showing S-opsin$^+$cones in the retina of a control mouse (drinking GES-free water). (**B**) Microphotograph from the retina in (**A**) showing S-cone outer segments. (**C**) Isodensity map from the retina in (**A**) showing the topography of S-opsin$^+$cones in the albino mouse. (**D**) Representative isodensity map showing the S-opsin$^+$cone distribution in a retina from a GES-treated mouse. Density color scale ranges from 0 (*purple*) to 18,000 or higher S$^+$ cones/mm^2 (*red*). *Bar*, 1 mm. (**E**) Graph showing the total number of S-opsin$^+$ cones in control and GES-treated mice. Data are shown as the mean number ± SEM of S$^+$ cones.

Investigative Ophthalmology & Visual Science

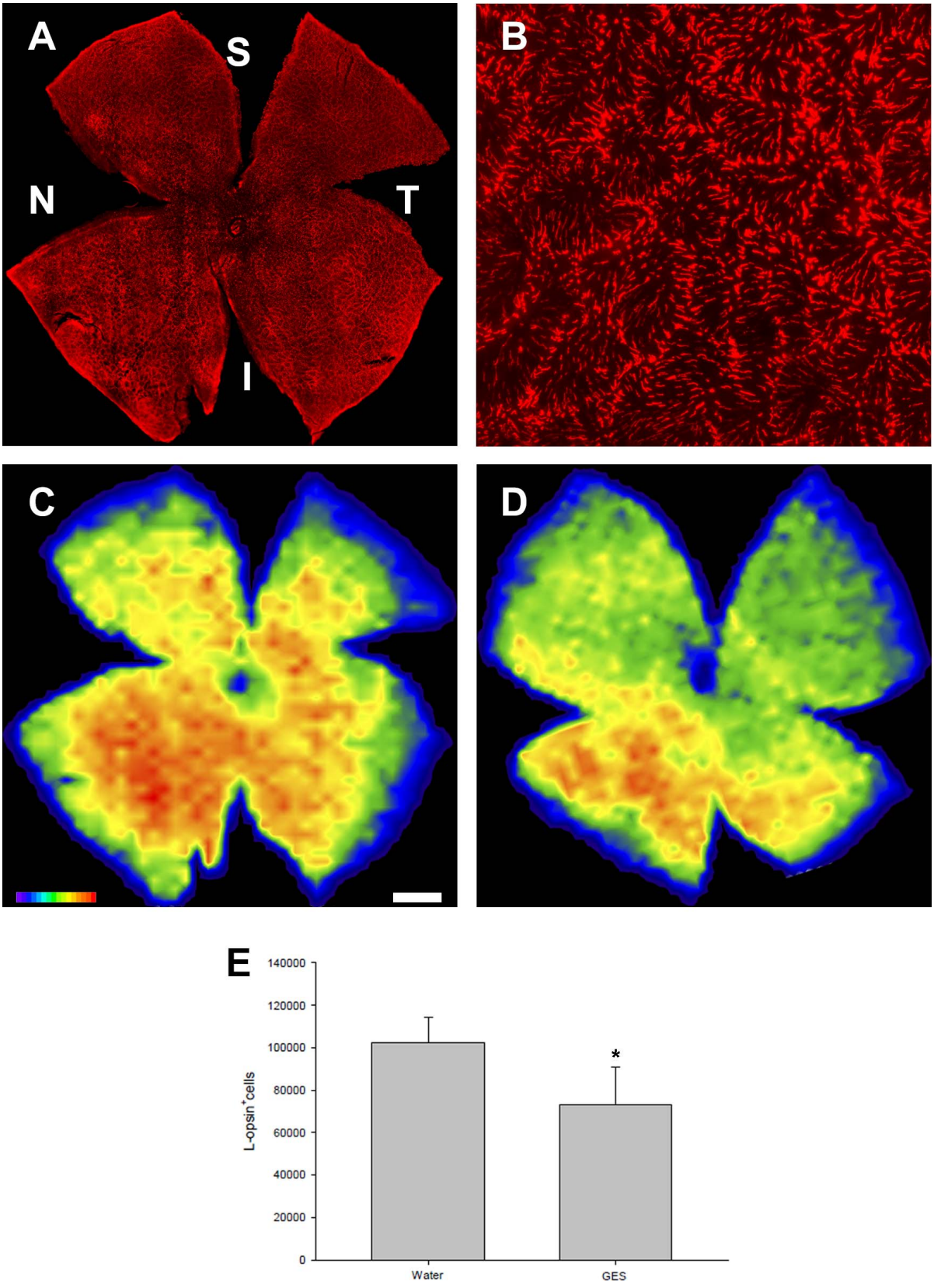

FIGURE 5. Loss of L-opsin$^+$cones in taurine depleted mice. (**A**) Representative retina showing L-opsin$^+$ cones in the retina of a control mouse (drinking GES-free water). (**B**) Microphotograph from the retina in (**A**) showing L-cone outer segments. (**C**) Isodensity map from the retina in (**A**) showing the topography of L-opsin$^+$cones in the albino mouse. (**D**) Representative isodensity map showing the L-opsin$^+$cone distribution in the right retina from a GES-treated mouse. Density color scale ranges from 0 (*purple*) to 16,000 or higher M-opsin$^+$ cones/mm^2 (*red*). *Bar*, 1 mm. (**E**) Graph showing the total number of L-opsin$^+$cones in control and GES-treated mice. Data are shown as the mean number ± SEM of M$^+$ cones.

Investigative Ophthalmology & Visual Science

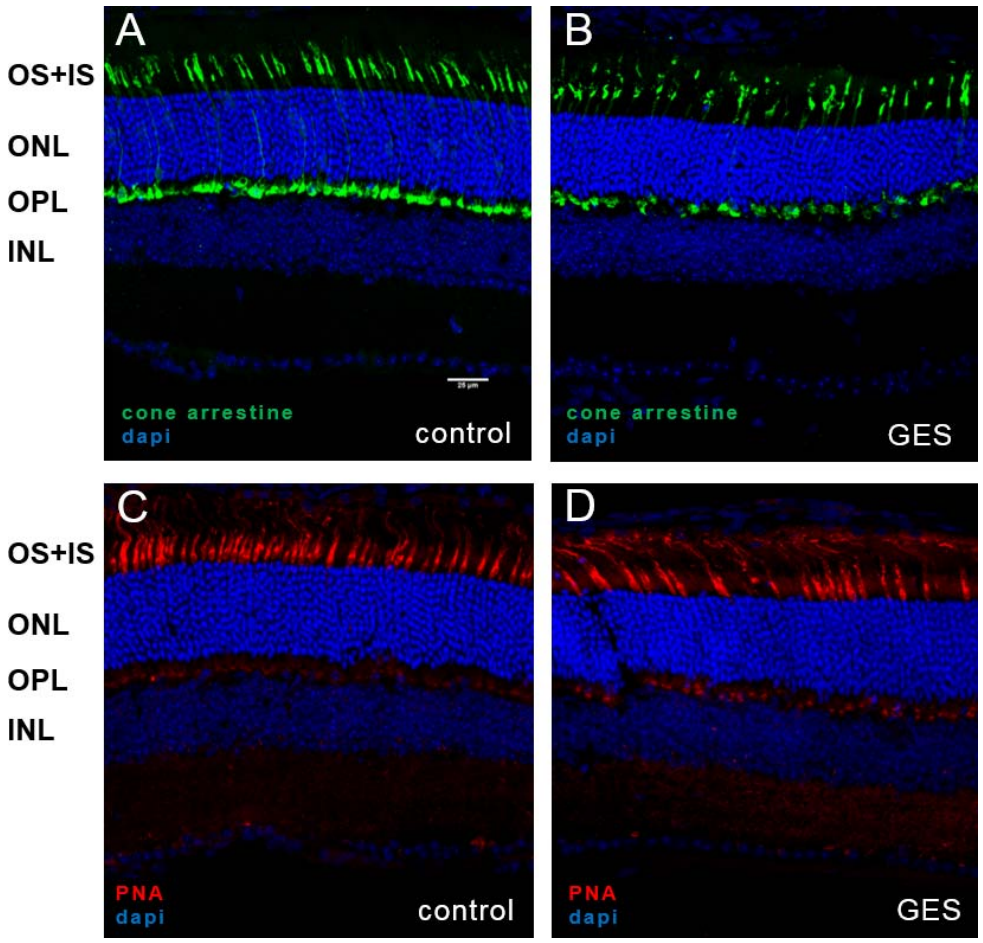

FIGURE 6. Changes in cone retinal morphology. Representative retinal cross-sections from a control (**A**, **C**) and a GES-treated mice (**B**, **D**) immunolabed against cone-arrestine (*green*; **A**, **B**) and stained for peanut lectin (*red*; **C**, **D**). Note the change in the morphology of cone outer segments and of cone synaptic terminals immunolabed by cone arrestine in GES-treated animals (**B**). OS, outer segments; IS, inner segments; INL, inner nuclear layer. The *scale bar* represents 25 μm.

previously observed by OCT. Even, the number of cell rows in the outer nuclear layer (ONL) was unchanged consistent with an absence of major rod photoreceptor loss. These observations are consistent with an earlier alteration of cone photoreceptors in GES-treated animals.

Total Population and Spatial Distribution of Brn3a$^+$RGCs

We previously reported that RGCs degenerate under taurine depletion but this was only shown on retinal sections.[19] Here, we examined the distribution of Brn3a$^+$ RGCs in the control and GES-treated animals. Brn3a$^+$ RGCs were denser in the central retina with a higher density of RGC above the optic nerve (Fig. 7A, 7C). We observed a decrease in the warm colors on the isodensity maps for the GES-treated animals (Fig. 7D), which seemed to be distributed throughout the entire retina. When quantified throughout the whole retina, Brn3a$^+$RGCs were decreased by 12% in GES-treated animals relative to nontreated controls (Fig. 7D; control: 44,049 ± 1505 RGCs, $n = 12$; GES-treated: 38,411 ± 4457 RGCs, $n = 12$). This difference was statistically significant ($P < 0.05$). The total number of Brn3a$^+$ RGCs found in the control retinas is in accordance with previously published data,[33,34] and indicates that the loss of RGCs was less severe than that of cone cells.

DISCUSSION

We have characterized, for the first time, the damaging effect of taurine depletion on the entire population of RGCs, S-opsin and L-opsin$^+$ cones in the mouse retina. Taurine depletion was verified by measuring taurine in plasma, confirming that chronic treatment with GES, a structural analog of taurine, causes a significant decrease in plasma taurine levels.[19] Guanidoethane sulfonate administration has been previously shown to decrease taurine levels in the heart, liver, and cerebellum.[35]

Taurine Depletion Causes Cone Loss in the Mouse Retina

It has been widely accepted that taurine plays an important role in photoreceptor survival since the 1970s when cats fed a taurine-free diet were found to become blind.[1] Subsequent studies confirmed photoreceptor degeneration in taurine-depleted animals using pharmacological strategies, a taurine free diet, or genetic knockout of the taurine transporter. However, these studies did not investigate which cell type was more sensitive to taurine depletion.[16,17,36] In our first paper on vigabatrin-induced retinal toxicity, we reported that cone degeneration appears earlier than rod lesions.[23] The subsequent demonstration of taurine depletion in vigabatrin-treated animals[9] showed that the sequential degeneration of cones,

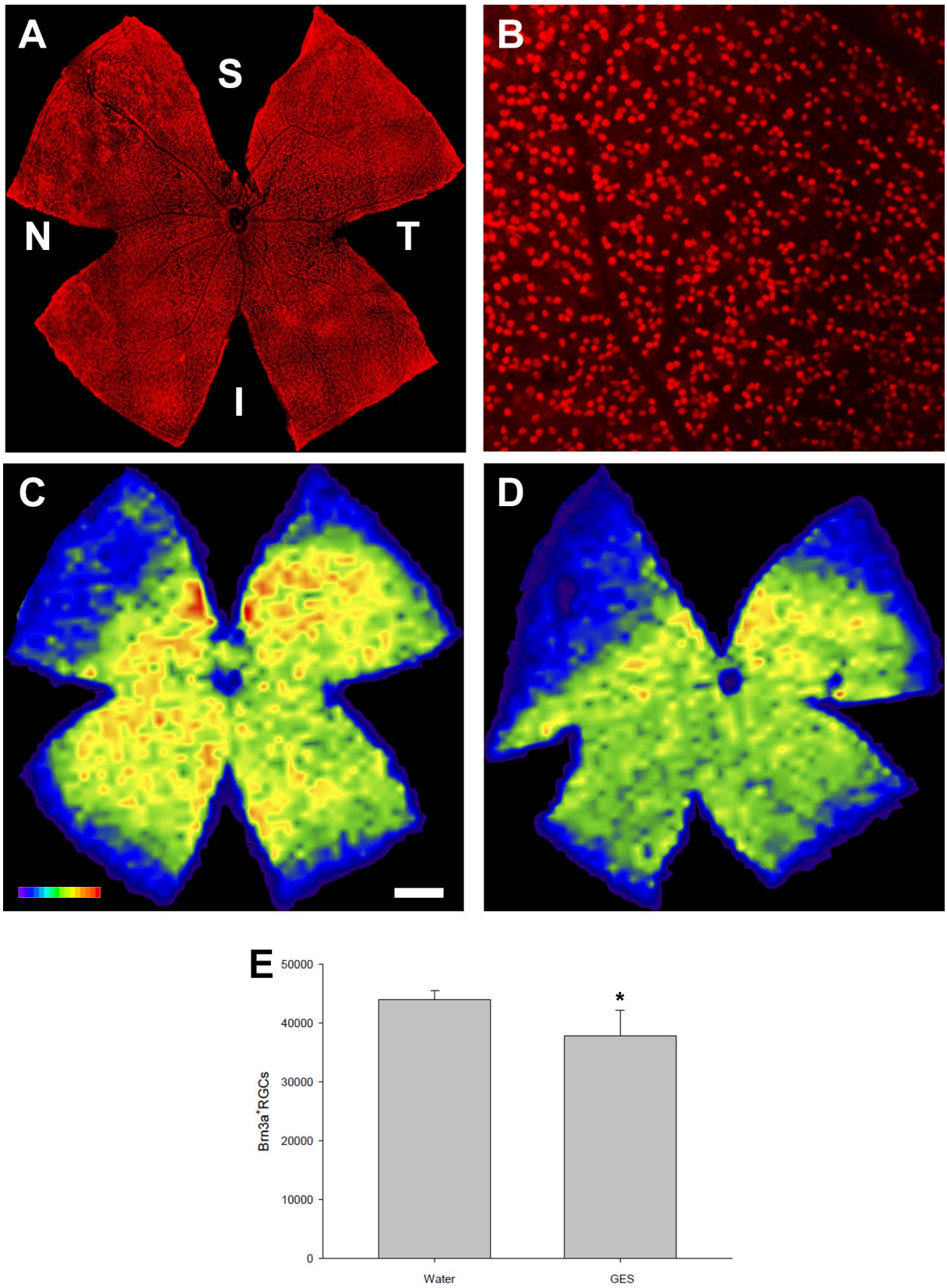

FIGURE 7. Loss of RGCs in taurine depleted mice. (**A**) Representative retina showing Brn3a$^+$RGCs in the retina of a control mouse (drinking GES-free water). (**B**) Microphotograph from the retina in (**A**) showing Brn3a$^+$RGCs. (**C**) Isodensity map from the retina in (**A**) showing the topography of Brn3a$^+$RGCs in the albino mouse. (**D**) Representative isodensity map showing the Brn3a$^+$RGC distribution in a retina from a mouse treated with GES. Density color scale ranges from 0 (*purple*) to 4800 or higher Brn3a$^+$RGCs/mm^2 (*red*). *Bar*, 1 mm. (**E**) Graph showing the total number of RGCs in control and GES-treated mice. Data are shown as the mean number ± SEM of RGCs.

Investigative Ophthalmology & Visual Science

followed by that that of rods, is a feature of taurine depletion. Thus, in the present study, we similarly demonstrated an earlier cone degeneration with apparently no rod degeneration. However, the dysfunction of rod photoreceptors is demonstrated by the reduction of scotopic ERG a-wave amplitudes. The greater reduction of both the photopic and flicker ERG measurements is consistent with a greater effect of taurine depletion on the cone pathway. This confirms that taurine deficiency induces retinal dysfunction in the cone pathway, as previously described by our group.[19] Here, we demonstrate a decrease in the total cone population using our recently described methods that allow us to count the total cone population and visualize their spatial distribution.[30] This confirms our previous results based on retinal sections.[19] In this previous study, retinal morphology was analyzed and disorganizations of the ONL, as well as changes in bipolar cells were described.[19] We observed that S-opsin$^+$ cones were more affected than L-opsin$^+$ cones. Greater degeneration of S-opsin$^+$ cones has also been reported in an animal model of Leber congenital amaurosis,[37] but the degenerative mechanism appears to be related to protein mistrafficking and endoplasmic reticulum stress, whereas taurine depletion may instead be related to an increase in oxidative stress and light damage.

Previous studies have suggested that S-opsin$^+$ cones are more sensitive to light damage than L-opsin$^+$ cones.[32,37] In addition, it is known that taurine depletion acts synergistically with light to induce photoreceptor loss.[20–22] This synergistic effect suggests that taurine depletion is likely to affect photoreceptor survival by decreasing their sensitivity threshold to light damage. S-opsin$^+$ cones are naturally more sensitive to taurine depletion because they are more sensitive to light damage (Glosmann M, et al. *IOVS* 2007;48:ARVO E-Abstract 1343).[32] This effect on the threshold to light damage may explain why retinal lesions are only seen in albino rodents. Indeed, the retinas of albino mice receive 70-fold more light than those of pigmented animals.[38] Daily light exposition can thus induce photoreceptor degeneration within a few months in taurine-depleted albino rodents, despite very low light levels in animal facilities. The limitation of light exposure by eye pigmentation may explain why several years are required to induce cone dysfunction in vigabatrin-treated patients, despite higher light exposition under natural conditions.[39] Our observation of preferential S-opsin$^+$ cone loss in GES-treated mice is consistent with the color vision dysfunction exhibited by vigabatrin-treated patients with a greater alteration of blue sensitivity.[40] This study suggests that taurine supplementation may provide neuroprotection in diseases of photoreceptor loss with earlier S-opsin$^+$ cone degeneration.

To confirm that taurine deficiency affects retinal function, scotopic and photopic ERGs were performed, showing that taurine deficiency causes a reduction in both ERG patterns. However, further studies are needed to correlate the respective cell losses of the different cone populations to specific ERG recordings measured using different wavelengths of light stimulation.

Taurine Depletion Causes RGC Loss in the Mouse Retina

In early experiments on taurine depletion, RGC loss and optic nerve fiber reduction were reported in addition to the massive loss of photoreceptors in GES-treated animals.[41] It was suggested that RGC loss was secondary to photoreceptor degeneration, as in retinal dystrophies, regardless of the etiology of the degeneration, whether inherited[42–44] or induced by phototoxicity.[24,25] However, secondary RGC degeneration is highly delayed relative to photoreceptor loss. Retinal ganglion cell loss in taurine-depleted animals occurs in parallel to cone photoreceptor degeneration,[18,19] whereas RGC loss in retinal dystrophies begins after the almost complete loss of photoreceptors.[25,44] Here, we further demonstrate that taurine depletion induced degeneration of the RGC population is parallel to that of the cone populations. Moreover, the cone losses are greater than the RGC loss. We also show that RGC loss is homogenous throughout the entire retina whereas the loss of cones appears to be greater in the dorsal retina. These results were obtained by counting the entire RGC population on flat-mounted retina using our previously described technique (please see references above). Retinal ganglion cells were identified by Brn3a immunolabeling because it labels the vast majority of RGCs in rodents.[29,45,46] The observed RGC loss was confirmed by the reduction of scotopic ERG b-wave amplitudes indicative of RGC dysfunction. Indeed, a reduction in b-wave amplitude was also reported in different animal models of glaucoma even with minor RGC loss.[47–49] A direct insult to RGCs under conditions of taurine depletion is also supported by a histopathological study of the retina from a vigabatrin-treated patient suggesting that RGCs were the primary site of the lesion.[11] Indeed, we have shown that pure RGCs survive better in culture with the addition of taurine in the medium,[49] consistent with the notion that in vivo taurine depletion can directly induce RGC degeneration. This RGC loss is consistent with the RGC degeneration observed in vigabatrin-treated animals also exhibiting taurine depletion.[18] The homogeneous cell loss across the retina observed in the present study suggests that similar homogeneous RGC degeneration occurs in vigabatrin-treated animals. This is strikingly different from the greater dorsal lesions of the photoreceptor layer.[23] This difference may reveal different degenerative mechanisms or cell sensitivities to oxidative stress across retinal tissue. Cone cell degeneration in taurine-depleted animals appears to be related to light damage as shown by the synergistic effect of light and taurine depletion.[20–22] Although RGC are not expected to be sensitive to light, many reports have demonstrated that oxidative stress is a key component of RGC dysfunction and degeneration in retinal diseases such as glaucoma.[50] However, some reports provide evidence for light damage in RGC models suggesting that these cells could also be sensitive to light damage when deprived of antioxidants, such as taurine.[6,51,52] This is consistent with the demonstration of oxidative stress as a major contributor to RGC degeneration during glaucoma.[50] A decrease in antioxidant defense is suggested, for example, by the decrease of blood levels of the antioxidant, glutathione, in primary open-angle and normal-tension glaucoma patients.[53]

Further studies are needed to demonstrate the role of light in RGC degeneration under conditions of antioxidant deprivation.

To our best knowledge, this is the first time that the total populations of RGCs and both types of cones (both L and S) have been studied in details in the taurine-depleted retina. Here, we show a higher affectation of the S-cone population than the L-cone population. It remains unclear if this greater S-cone loss is related to their short wavelength and blue sensitivity because blue light is particularly phototoxic,[54,55] and/or because blue S-cones appear more sensitive to oxidative stress.

In summary, we confirm that taurine depletion causes RGC and cone (both L- and S-cones) degeneration. Moreover, we establish, for the first time, a gradient of retinal cell loss in taurine depleted mice as follows: (1) S-opsin$^+$ cones, (2) L-opsin$^+$ cones, and (3) RGCs. This gradient suggests that different mechanisms may be responsible for cellular degeneration and that susceptibility to light damage may play a role in determining this pattern of degeneration. Further studies are

needed to clarify the role of light in retinal degeneration under taurine deprivation.

Acknowledgments

Supported by grants from Spanish Ministry of Economy and Competitivenes (Spain): SAF-2015-67643; Instituto de Salud Carlos III-FEDER "Una manera de hacer Europa" (Spain) PI13/00643, PI13/01266, Redes temáticas de investigación cooperativa en salud (RETICS, Spain): RD12/0034/0014, Ministerio de Educación, Cultura y Deporte (Spain): CAS14/00188. By Institut national de la santé et de la recherche médicale (INSERM; France), Université Pierre et Marie CURIE (UPMC; Paris VI; France), the city of Paris, the Regional Council of Ile-de-France, the LabEx LIFESENSES (ANR-10-LABX-65), which was supported by French state funds managed by the ANR within the Investissements d'Avenir programme (ANR-11-IDEX-0004-02) and by the program Light4Deaf, which is also part of the French state funds managed by the ANR within the Investissements d'Avenir programme under reference ANR-15-RHUS-0001.

Disclosure: **W. Hadj-Saïd**, None; **N. Froger**, None; **I. Ivkovic**, None; **M. Jiménez-López**, None; **É. Dubus**, None; **J. Dégardin-Chicaud**, None; **M. Simonutti**, None; **C. Quénol**, None; **N. Neveux**, None; **M.P. Villegas-Pérez**, None; **M. Agudo-Barriuso**, None; **M. Vidal-Sanz**, None; **J.-A. Sahel**, None; **S. Picaud**, None; **D. García-Ayuso**, None

References

1. Hayes KC, Carey RE, Schmidt SY. Retinal degeneration associated with taurine deficiency in the cat. *Science*. 1975; 188:949–951.
2. Pasantes-Morales H, Quiroz H, Quesada O. Treatment with taurine diltiazem, and vitamin E retards the progressive visual field reduction in retinitis pigmentosa: a 3-year follow-up study. *Metab Brain Dis*. 2002;17:183–197.
3. Orr HT, Cohen AI, Carter JA. The levels of free taurine, glutamate, glycine and gamma-amino butyric acid during the postnatal development of the normal and dystrophic retina of the mouse. *Exp Eye Res*. 1976;23:377–384.
4. Schmidt SY, Berson EL. Taurine uptake in isolated retinas of normal rats and rats with hereditary retinal degeneration. *Exp Eye Res*. 1978;27:191–198.
5. Airaksinen EM, Sihvola P, Airaksinen MM, Sihvola M, Tuovinen E. Uptake of taurine by platelets in retinitis pigmentosa. *Lancet*. 1979;1:474–475.
6. Froger N, Moutsimilli L, Cadetti L, et al. Taurine: the comeback of a neutraceutical in the prevention of retinal degenerations. *Prog Retin Eye Res*. 2014;41C:44–63.
7. Geggel HS, Ament ME, Heckenlively JR, Martin DA, Kopple JD. Nutritional requirement for taurine in patients receiving long-term parenteral nutrition. *N Engl J Med*. 1985;312:142–146.
8. Ament ME, Geggel HS, Heckenlively JR, Martin DA, Kopple J. Taurine supplementation in infants receiving long-term total parenteral nutrition. *J Am Coll Nutr*. 1986;5:127–135.
9. Jammoul F, Wang Q, Nabbout R, et al. Taurine deficiency is a cause of vigabatrin-induced retinal phototoxicity. *Ann Neurol*. 2009;65:98–107.
10. Eke T, Talbot JF, Lawden MC. Severe persistent visual field constriction associated with vigabatrin. *BMJ*. 1997;314:180–181.
11. Ravindran J, Blumbergs P, Crompton J, Pietris G, Waddy H. Visual field loss associated with vigabatrin: pathological correlations. *J Neurol Neurosurg Psychiatry*. 2001;70:787–789.
12. Frisen L, Malmgren K. Characterization of vigabatrin-associated optic atrophy. *Acta Ophthalmol Scand*. 2003;81:466–473.
13. Buncic JR, Westall CA, Panton CM, Munn JR, MacKeen LD, Logan WJ. Characteristic retinal atrophy with secondary "inverse" optic atrophy identifies vigabatrin toxicity in children. *Ophthalmology*. 2004;111:1935–1942.
14. Wild JM, Robson CR, Jones AL, Cunliffe IA, Smith PE. Detecting vigabatrin toxicity by imaging of the retinal nerve fiber layer. *Invest Ophthalmol Vis Sci*. 2006;47:917–924.
15. Neuringer M, Sturman J. Visual acuity loss in rhesus monkey infants fed a taurine-free human infant formula. *J Neurosci Res*. 1987;18:597–601.
16. Lake N, Malik N. Retinal morphology in rats treated with a taurine transport antagonist. *Exp Eye Res*. 1987;44:331–346.
17. Heller-Stilb B, van Roeyen C, Rascher K, et al. Disruption of the taurine transporter gene (taut) leads to retinal degeneration in mice. *FASEB J*. 2002;16:231–233.
18. Jammoul F, Degardin J, Pain D, et al. Taurine deficiency damages photoreceptors and retinal ganglion cells in vigabatrin-treated neonatal rats. *Mol Cell Neurosci*. 2010;43:414–421.
19. Gaucher D, Arnault E, Husson Z, et al. Taurine deficiency damages retinal neurones: cone photoreceptors and retinal ganglion cells. *Amino Acids*. 2012;43:1979–1993.
20. Rapp LM, Thum LA, Anderson RE. Synergism between environmental lighting and taurine depletion in causing photoreceptor cell degeneration. *Exp Eye Res*. 1988;46:229–238.
21. Cocker SE, Lake N. Effects of dark maintenance on retinal biochemistry and function during taurine depletion in the adult rat. *Vis Neurosci*. 1989;3:33–38.
22. Rascher K, Servos G, Berthold G, et al. Light deprivation slows but does not prevent the loss of photoreceptors in taurine transporter knockout mice. *Vision Res*. 2004;44:2091–2100.
23. Duboc A, Hanoteau N, Simonutti M, et al. Vigabatrin, the GABA-transaminase inhibitor, damages cone photoreceptors in rats. *Ann Neurol*. 2004;55:695–705.
24. Marco-Gomariz MA, Hurtado-Montalban N, Vidal-Sanz M, Lund RD, Villegas-Perez MP. Phototoxic-induced photoreceptor degeneration causes retinal ganglion cell degeneration in pigmented rats. *J Comp Neurol*. 2006;498:163–179.
25. Garcia-Ayuso D, Salinas-Navarro M, Agudo-Barriuso M, Alarcón-Martínez L, Vidal-Sanz M, Villegas-Pérez MP. Retinal ganglion cell axonal compression by retinal vessels in light-induced retinal degeneration. *Mol Vis*. 2011;17:1716–1733.
26. Berger A, Cavallero S, Dominguez E, et al. Spectral-domain optical coherence tomography of the rodent eye: highlighting layers of the outer retina using signal averaging and comparison with histology. *PLoS One*. 2014;9:e96494.
27. Berson EL. Retinitis pigmentosa and allied retinal diseases: electrophysiologic findings. *Trans Sect Ophthalmol Am Acad Ophthalmol Otolaryngol*. 1975;81(pt 1):OP659–OP666.
28. Neveux N, David P, Cynober L. Measurement of amino acid concentration in biological fluids and tissues using ion-exchange chromatography. In: Cynober LA, ed. *Metabolic & Therapeutic Aspects of Amino Acids in Clinical Nutrition*. 2nd ed. Boca Raton, FL: CRC Press; 2004:17–28.
29. Nadal-Nicolas FM, Jimenez-Lopez M, Sobrado-Calvo P, et al. Brn3a as a marker of retinal ganglion cells: qualitative and quantitative time course studies in naive and optic nerve-injured retinas. *Invest Ophthalmol Vis Sci*. 2009;50:3860–3868.
30. Ortín-Martínez A, Nadal-Nicolás FM, Jiménez-López M, et al. Number and distribution of mouse retinal cone photoreceptors: differences between an albino (Swiss) and a pigmented (C57/BL6) strain. *PLoS One*. 2014;9:102392.
31. Ortín-Martínez A, Jiménez-López M, Nadal-Nicolás FM, et al. Automated quantification and topographical distribution of the whole population of S-and L-cones in adult albino and

pigmented rats. *Invest Ophthalmol Vis Sci*. 2010;51:3171–3183.

32. Ortín-Martínez A, Valiente-Soriano FJ, García-Ayuso D, et al. A novel in vivo model of focal light emitting diode-induced cone-photoreceptor phototoxicity: neuroprotection afforded by brimonidine, BDNF, PEDF or bFGF. *PLoS One*. 2014;9:e113798.
33. Salinas-Navarro M, Jiménez-López M, Valiente-Soriano FJ, et al. Retinal ganglion cell population in adult albino and pigmented mice: a computerized analysis of the entire population and its spatial distribution. *Vision Res*. 2009;49:637–647.
34. Valiente-Soriano FJ, García-Ayuso D, Arturo O-M, et al. Distribution of melanopsin positive neurons in pigmented and albino mice: evidence for melanopsin interneurons in the mouse retina. *Front Neuroanat*. 2014;8:131.
35. Huxtable RJ, Laird HE, II Lippincott SE. The transport of taurine in the heart and the rapid depletion of tissue taurine content by guanidinoethyl sulfonate. *J Pharmacol Exp Ther*. 1979;211:465–471.
36. Imaki H, Moretz R, Wisniewski H, Neuringer M, Sturman J. Retinal degeneration in 3-month-old rhesus monkey infants fed a taurine-free human infant formula. *J Neurosci Res*. 1987;18:602–614.
37. Zhang T, Zhang N, Baehr W, Fu Y. Cone opsin determines the time course of cone photoreceptor degeneration in Leber congenital amaurosis. *Proc Natl Acad Sci U S A*. 2011;108:8879–8884.
38. Lyubarsky AL, Daniele LL, Pugh EN, Jr. From candelas to photoisomerizations in the mouse eye by rhodopsin bleaching in situ and the light-rearing dependence of the major components of the mouse ERG. *Vision Res*. 2004;44:3235–3251.
39. Banin E, Shalev RS, Obolensky A, Neis R, Chowers I, Gross-Tsur V. Retinal function abnormalities in patients treated with vigabatrin. *Arch Ophthalmol*. 2003;121:811–816.
40. Nousiainen I, Kalviainen R, Mantyjarvi M. Color vision in epilepsy patients treated with vigabatrin or carbamazepine monotherapy. *Ophthalmology*. 2000;107:884–888.
41. Lake N, Malik N, De Marte L. Taurine depletion leads to loss of rat optic nerve axons. *Vision Res*. 1988;28:1071–1076.
42. Marc RE, Jones BW. Retinal remodeling in inherited photoreceptor degenerations. *Mol Neurobiol*. 2003;28:139–147.
43. Villegas-Perez MP, Lawrence JM, Vidal-Sanz M, Lavail MM, Lund RD. Ganglion cell loss in RCS rat retina: a result of compression of axons by contracting intraretinal vessels linked to the pigment epithelium. *J Comp Neurol*. 1998;392:58–77.
44. García-Ayuso D, Salinas-Navarro M, Agudo M, et al. Retinal ganglion cell numbers and delayed retinal ganglion cell death in the P23H rat retina. *Exp Eye Res*. 2010;91:800–810.
45. Galindo-Romero C, Aviles-Trigueros M, Jimenez-Lopez M, et al. Axotomy-induced retinal ganglion cell death in adult mice: quantitative and topographic time course analyses. *Exp Eye Res*. 2011;92:377–387.
46. Vidal-Sanz M, Nadal-Nicolas FM, Valiente-Soriano FJ, Agudo-Barriuso M, Villegas-Perez MP. Identifying specific RGC types may shed light on their idiosyncratic responses to neuroprotection. *Neural Regen Res*. 2015;10:1228–1230.
47. Mittag TW, Danias J, Pohorenec G, et al. Retinal damage after 3 to 4 months of elevated intraocular pressure in a rat glaucoma model. *Invest Ophthalmol Vis Sci*. 2000;41:3451–3459.
48. Fortune B, Bui BV, Morrison JC, et al. Selective ganglion cell functional loss in rats with experimental glaucoma. *Invest Ophthalmol Vis Sci*. 2004;45:1854–1862.
49. Froger N, Cadetti L, Lorach H, et al. Taurine provides neuroprotection against retinal ganglion cell degeneration. *PLoS One*. 2012;7:e42017.
50. Tezel G. Oxidative stress in glaucomatous neurodegeneration: mechanisms and consequences. *Prog Retin Eye Res*. 2006;25:490–513.
51. Li GY, Osborne NN. Oxidative-induced apoptosis to an immortalized ganglion cell line is caspase independent but involves the activation of poly(ADP-ribose)polymerase and apoptosis-inducing factor. *Brain Res*. 2008;1188:35–43.
52. del Olmo-Aguado S, Nunez-Alvarez C, Ji D, Manso AG, Osborne NN. RTP801 immunoreactivity in retinal ganglion cells and its down-regulation in cultured cells protect them from light and cobalt chloride. *Brain Res Bull*. 2013;98:132–144.
53. Gherghel D, Mroczkowska S, Qin L. Reduction in blood glutathione levels occurs similarly in patients with primary-open angle or normal tension glaucoma. *Invest Ophthalmol Vis Sci*. 2013;54:3333–3339.
54. Roberts JE. Ocular phototoxicity. *J Photochem Photobiol B*. 2001;64:136–143.
55. Arnault E, Barrau C, Nanteau C, et al. Phototoxic action spectrum on a retinal pigment epithelium model of age-related macular degeneration exposed to sunlight normalized conditions. *PLoS One*. 2013;8:e71398.

Investigative Ophthalmology & Visual Science